American Industrial Hygiene Association Journal

ISSN: 0002-8894 (Print) (Online) Journal homepage: https://www.tandfonline.com/loi/aiha20

PRELIMINARY EVALUATION OF AN ACTIVE END-OF-SERVICE-LIFE INDICATOR FOR ORGANIC VAPOR CARTRIDGE RESPIRATORS

Ernest S. Moyer , M.W. Findlay , G.J. Maclay & J.R. Stetter

To cite this article: Ernest S. Moyer , M.W. Findlay , G.J. Maclay & J.R. Stetter (1993) PRELIMINARY EVALUATION OF AN ACTIVE END-OF-SERVICE-LIFE INDICATOR FOR ORGANIC VAPOR CARTRIDGE RESPIRATORS, American Industrial Hygiene Association Journal, 54:8, 417-425, DOI: 10.1080/15298669391354900

To link to this article: https://doi.org/10.1080/15298669391354900

Preliminary Evaluation of an Active End-of-Service-Life Indicator for Organic Vapor Cartridge Respirators

Ernest S. Moyer[a]
M.W. Findlay[b]
G.J. Maclay[b]
J.R. Stetter[b]

[a]National Institute for Occupational Safety and Health, Division of Safety Research, Protective Technology Branch, Respiratory Protection Section, 944 Chestnut Ridge Road, Morgantown, West Virginia 26505; [b]Transducer Research, Inc., 999 Chicago Avenue, Naperville, Illinois 60540

Data are presented on a microwatt chemiresistor microsensor for use with negative-pressure organic vapor respirators. This sensor would operate at or within a sorbent bed and detect parts per million levels of chemical vapors and/or gases as a function of sensor resistance. Sensors were evaluated against four challenge concentrations of ethyl acetate (750 ppm, 1000 ppm, 1500 ppm, and 2000 ppm). Direct comparison of breakthrough times and curves for the chemiresistor microsensor and a standard infrared (IR) detector system were made. The chemiresistor sensor responses were found to correlate well with the IR system. The evaluation showed that although the chemiresistor sensors were not as sensitive as the IR detectors, they could be used if located inside the charcoal bed. Thus, these sensors could function as organic-vapor detectors and could be used in cartridge applications. However, further improvements in stability and sensitivity of these chemiresistor sensors is necessary.

Negative-pressure air-purifying respirators are used to protect wearers against particulates, gases, and vapors. The gas/vapor-type respirators are designed for use against acid gas, ammonia, carbon monoxide, organic vapors, and other special contaminants like vinyl chloride (Title 30, *Code of Federal Regulations*, Part 11 § 11.200). These negative-pressure organic-vapor (OV) respirators have use limitations imposed on them. In particular, 30 CFR Part 11 Subpart I (Gas Masks) and Subpart L (Chemical Cartridge Respirators) footnote these limitations. The single most restrictive use limitation is the following: "Not for use against gases or vapors with poor warning properties (except where MSHA or Occupational Safety and Health Administration standards permit use for a specific gas or vapor) or those which generate high heats of reaction with sorbent materials in the canister."[1] This same limitation applies to chemical cartridge respirators (30 CFR Part 11 Subpart L § 11.150) with an added stipulation that "maximum use concentrations are lower for organic vapors which produce atmospheres immediately hazardous to life or health at concentrations equal to or lower than this concentration,"[2] which is 1000 ppm for organic vapor.

Because many gases/vapors do not possess adequate warning properties, the use of negative-pressure respirators against organic vapors is very limited. Warning properties could include odor threshold, eye irritation, respiratory tract irritation, and/or taste. The recognized definition for adequate warning properties means that a gas or vapor has a persistent odor or irritant effect at concentrations at or below the Occupational Safety and Health Administration (OSHA) permissible exposure level (PEL) or National Institute for Occupational Safety and Health (NIOSH) recommended exposure limit (REL).[3] Mixtures where interactions can affect warning properties complicate matters. Thus, the reliance on adequate warning properties of environmental contaminants is the most significant problem associated with the use of OV cartridge respirators. In fact, the NIOSH Respirator Decision Logic states "no physiological effects in humans (e.g., odor, taste, eye irritation, respiratory irritation) have been demonstrated as being capable of consistently providing respirator wearers with timely, consistent, persistent, and reliable warning of hazardous airborne concentrations inside a respirator . . . . Warning properties should be regarded with caution and with recognition of their unreliability."[3] Reviews of some of these issues appear in the literature.[4–6]

The above-mentioned limitations had to be adopted because of the difficulty of predicting breakthrough times for

The work at Transducer Research, Inc., was funded by CDC/NIOSH under Grant #5R44.OH02312-03.

Disclaimer: Mention of a company name or product does not constitute endorsement by the National Institute for Occupational Safety and Health (NIOSH).

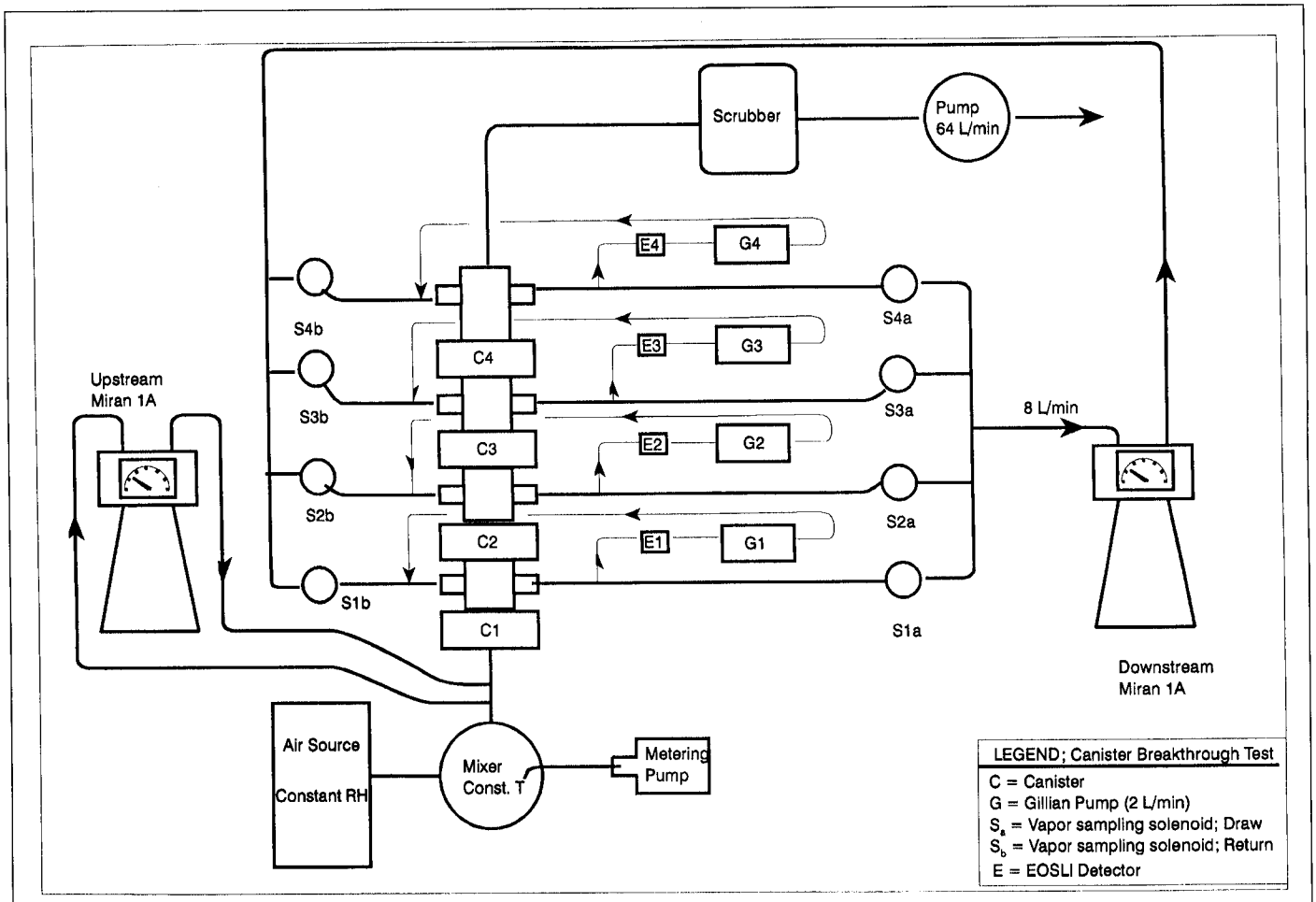

FIGURE 1. Experimental apparatus for simultaneous monitoring of infrared and microsensor ethyl acetate breakthrough

diverse contaminants and environmental conditions observed in the workplace. Further, effective end-of-service-life indicators (EOSLI) have not been developed to monitor cartridge breakthrough of organic contaminants. Development of an effective EOSLI would make reliance on adequate warning properties unnecessary while still providing workers using OV cartridge respirators with adequate warning against exposure to toxic substances. Thus, an effective active EOSLI needs to be developed to provide a reliable means of sensing OV breakthrough and to remove reliance on human senses. Human senses are not foolproof, vary greatly from individual to individual, and can change depending on an individual's medical status.

This article deals with the evaluation of microsensors that might fill the void as active EOSLI. The sensors are microwatt chemiresistor microsensors,[7] which ultimately would operate at or within the sorbent beds and detect ppm levels of organic vapor and gas indicating the exhaustion of the carbonaceous adsorbent bed. The sensor must provide an unambiguous alarm (flashing LED) to the user when at least 10% of the respirator cartridge service life remains. Also, the device cannot interfere with the operation of the respirator. Further, goals of low cost and small size were imposed on the sensors. The sensors were evaluated at four challenge concentrations of ethyl acetate. Their responses are compared with that of an infrared (IR) detector.[8]

EXPERIMENTAL

The laboratory setup has been described previously.[8,9] The system was modified to place the sensor loop in parallel with the Miran® 1A infrared gas (IR) analyzer loop (The Foxboro Co., Foxboro, MA) and is shown in Figure 1. Further, the sensor loop was arranged so that each of the four sensors continually contacts a sample over the entire experimental run rather than being affected by the switching valves that control the IR sampling location. By this arrangement, data from both systems were collected and analyzed in a comparative fashion.

Modifications have been made to improve the OV test system's stability. A Laboratory Data Control Model 396 liquid chromatography mini-pump (Milton Roy, Riviera Beach, FL) replaced the syringe pump to feed solvent at a controlled, predetermined rate to the airstream. This modification allowed the buffer tank to be reduced to five gallons (18.9 L) and still maintain the inlet vapor concentration (C_o), which was continually monitored with a Miran 1A IR. Also, the buffer tank was wrapped with heating tape connected to a

variable power supply for improved temperature control.

The airstream (50% relative humidity for all tests) containing the challenge ethyl acetate vapor was pulled through the anodized aluminum cell housing, which contained four cartridges in series. This spacer arrangement allowed for the selection of cartridges in series to resemble a packed column of varying bed length and sorbent weight. Consecutive sampling of the downstream breakthrough vapor concentration (approximately 20% of complete curve) was performed by a Miran 1A IR, while the four separate sensor loops continuously monitored the breakthrough concentration over the entire experimental run. This was accomplished by placing one sensor downstream of each cartridge. When the IR was used to sample the generated atmosphere, a flow rate of 8 L/min was employed. A tee was inserted in line before each solenoid valve. An air pump (Gilian Instruments Corp., W. Caldwell, NJ) was employed to draw 2 L/min continually through each sensor. The flows were fed back to the cell in a closed-loop arrangement to maintain flow. This arrangement allowed four breakthrough curves to be obtained by each detector system during a single experimental run.

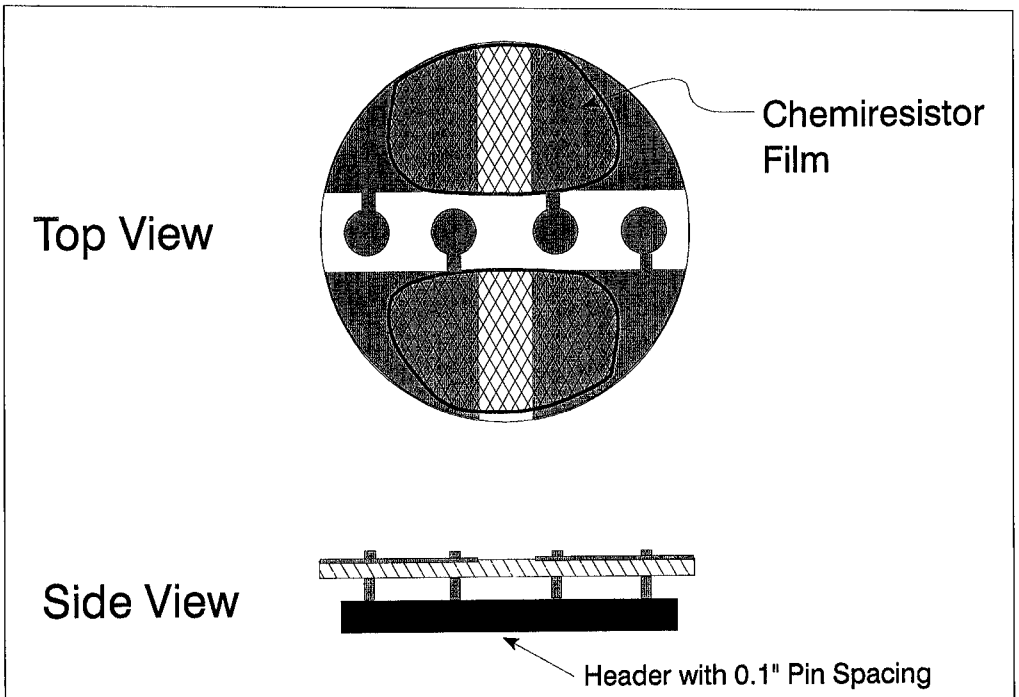

FIGURE 2. Illustration of fabricated EOSLI chemiresistor microsensor

After all the cartridges had shown breakthrough, the cell holder was removed and disassembled, and final weights were determined for the individual cartridges. Next, the sorbent was removed in order to obtain the weight of the empty cartridge case. From the initial weights and the above information, the amount of sorbent present in each cartridge and the amount of vapor adsorbed could be calculated. These data were then entered into the computer, which calculated the upstream and penetration vapor concentrations and printed out a copy of the four breakthrough curves (ppm versus time). These data were then stored on disk for future data analysis. Also, from the fill volume of the cartridge and the sorbent weight, a value for ρ_β, the bulk density of the packed bed (g/cm^3) was determined.

The ethyl acetate challenge concentrations used were 750 ppm, 1000 ppm, 1500 ppm, and 2000 ppm. The flow rate through the cartridges was set at 64 L/min by means of a dry test meter. The relative humidity was 50%, as controlled by a Miller-Nelson Research, Inc., Model HCS-201 flow temperature-RH control system, equipped with a General Eastern Model 400D % Relative Humidity/Temperature sensor, and verified at the cell entrance by an EG&G Model 911 DEW ALL Digital Humidity Analyzer. The temperature was 25 ± 2 °C.

MATERIALS

Ethyl acetate, purchased from Fisher Scientific (Fairlawn, NJ), was certified American Chemical Society spectranalyzed lot #902801.

House air was passed through a dryer, sorbent, and high efficiency filter to remove residual contaminants. This air was supplied to the Miller-Nelson Research Inc. Model HCS-201 control system.

The OV cartridges were all from a single lot of cartridges containing a coconut-base charcoal.

INFRARED DATE ACQUISITION SYSTEM (IR)

The upstream and downstream concentrations were monitored by two Miran 1A general purpose IR analyzers equipped with a variable pathlength gas cell. The analytical wavelength employed was 8.3 μm for ethyl acetate. The IR data collection was done automatically by means of a Hewlett-Packard (HP) Series 200 computer. An HP 3497A Data Acquisition System (DAS) was used to control the test instruments and collect the data. An eight-channel High Voltage Actuator card was used to control the valves so that the different sampling ports could be selected.

Sensors

These sensors are carbon/polymer film microsensors. The four sensors evaluated in this study were fabricated by Transducer Research Inc. from proprietary mixtures of silicone and Darco carbon. Each sensor is monitored for an increase in resistance as a function of exposure to organic vapors. The sensors probably function by taking up organic components that cause the elastomer to expand, thus

increasing the mean separation between carbon particles in the elastomer matrix. This expansion reduces the conductivity of the sensor material and is most likely due to a bulk mechanical swelling phenomena.

The sensors were made by spraying mixtures of activated Darco-60 carbon (Frederick G. Smith Co., Columbus, OH) and silicone rubber onto phenolic substrates with two etched copper electrodes. The film was built up so as to produce a resistance of approximately 10 000 ohms. Figure 2 depicts a top and side view of the devices. The resistance was determined with a Wheatstone bridge circuit, having a supply voltage of 6 volts. The output voltage of the bridge circuit was used to drive an LED alarm. The electronics basically consisted of a linear bridge that compared the sensor resistance to a reference value.[7] In this particular application, each sensor bridge circuit was calibrated and the outputs from the sensors (four total) were fed to a data logger for analysis.

The sensors could be located either inside the facepiece of the respirator, or within the cartridge bed. If the sensors are embedded in the cartridges, then they would be disposed of after use. However, use inside the facepiece might be optimal. In these studies, four sensors were employed for all the studies, with a steady-state baseline being determined before subsequent runs. In fact, these studies were performed to evaluate potential sensor sites and sensor characteristics including multiple use.

The sensor's signals were fed to a signal-processing module located on the respirator facepiece. This low-powered module activated a flashing LED alarm when the contaminant concentration reached a threshold value. The total device and associated electronics are projected to take up a volume of approximately 10–20 cm^3, weigh 25 grams, and cost about $3.00. They would not alter the normal operation or function of the respirator.

ANALYSIS

These experiments were conducted to determine how accurately the sensors detect breakthrough. Calculations were then performed using the experimental data to determine the best location for the sensor within the bed. The bed location

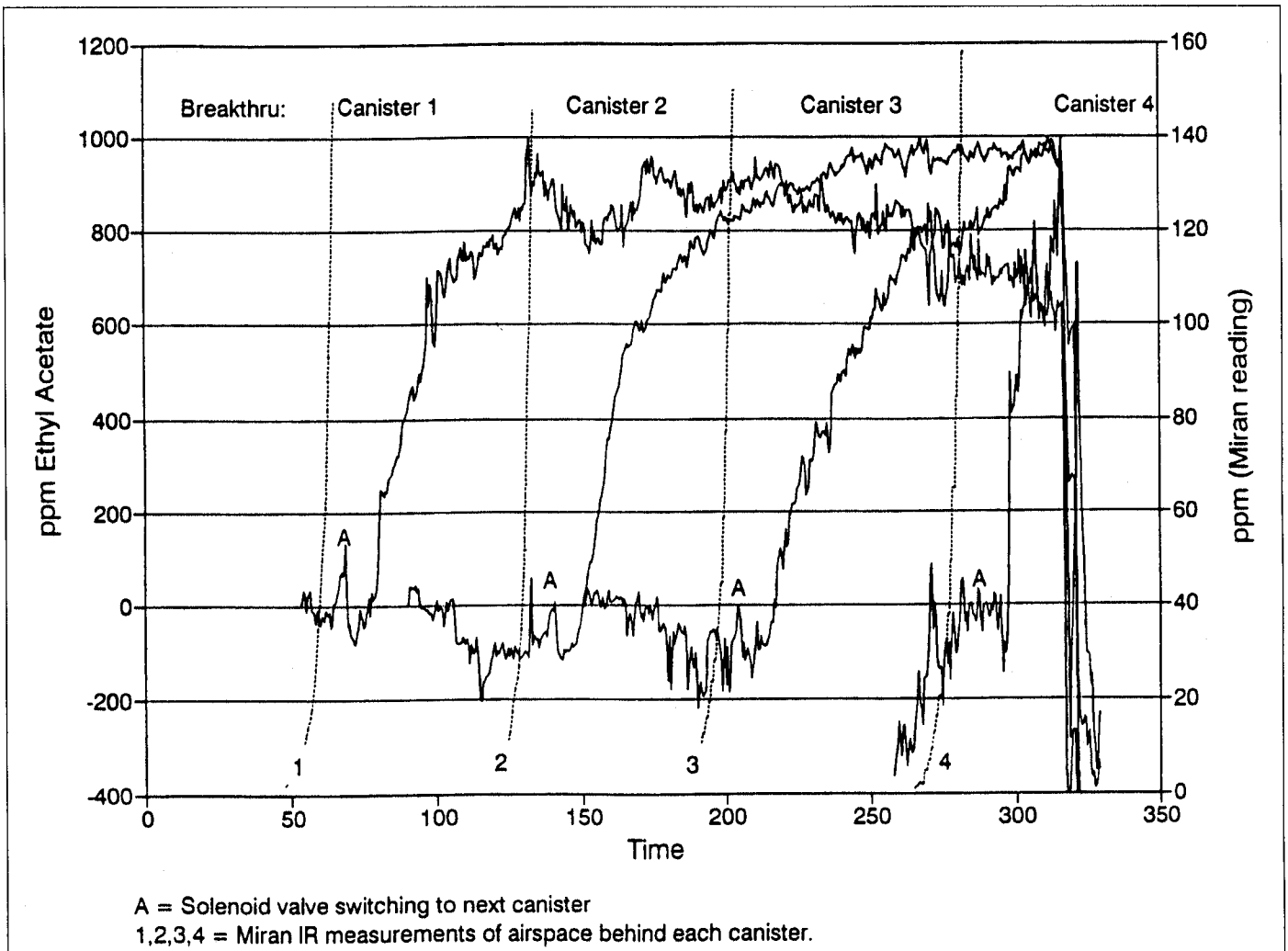

FIGURE 3. Breakthrough curves (concentration versus time) for microsensor response (left axis) and infrared detector response (right axis)

TABLE I. Organic Vapor Cartridge Breakthrough Time (t_b) Against 1000 ppm Ethyl Acetate for Stacked Cartridges[A]

Run #	Filter # in Stacked Array	Cumulative Charcoal WT (g)	IR t_b Corrected to 1000 ppm (min) at Various Penetration			t_b to Midpoint of Sensor Response (min)	W[B] Charcoal Bed Weight Needed for 100 ppm (g)	$W_{\%}$[C] % of Bed Where Sensor to be Located
			10 ppm	50 ppm	100 ppm			
1	1	70.948	54.8	61.2	64.1	87	53.9	76
	2	141.795	125.3	131.1	133.6	147	115.1	81
	3	212.112	193.9	201.0	203.9	220	177.1	84
	4	282.688	273.8	280.5	283.4	289	247.2	87
2	1	69.886	56.3	62.2	64.7	82	54.4	78
	2	140.377	127.8	133.9	136.5	177	117.7	84
	3	210.761	198.0	204.2	206.9	256	179.8	85
	4	281.550	273.4	280.0	282.2	286	246.1	87
3	1	64.555	51.1	57.3	59.8	78	50.1	78
	2	135.273	119.8	126.2	128.6	147	110.7	82
	3	205.281	191.7	198.3	200.9	252	174.5	85
	4	275.885	262.3	268.8	271.4	278	236.6	86

[A]Carbon Bed Density 0.44 g/cm^3

[B] $W = \frac{t_b - 2.9992}{1.134}$

[C] $W_{\%} = \frac{W}{W_{cum}}(100)$

should be such that approximately 10% of the service life remains, or that the exiting concentration is well below the substance's Recommended Exposure Level (REL). Naturally, the challenge concentration will have an effect on the adsorption profile in the bed and the breakthrough time and concentration.

A modified Wheeler equation (Equation 1) was used to calculate the sensor location within the sorbent bed. This equation indicates that the adsorption capacity and gas adsorption rate of a packed charcoal sorbent bed are described by the linear relationship between gas breakthrough time and sorbent weight. The modified Wheeler equation[10] is as follows:

$$t_b = \frac{w_e}{C_O Q}\left[W - \frac{\rho_\beta Q}{k_v}\mathrm{Ln}(C_O/C_X)\right] \quad (1)$$

where

t_b = breakthrough time (min);
C_x = exit concentration (g/cm^3);
C_o = inlet concentration (g/cm^3);
Q = volumetric flow rate (cm^3/min);
W = weight of adsorbent (g);
ρ_β = bulk density of the packed bed (g/cm^3);
W_e = adsorption capacity (g/g)
k_v = first order rate constant of adsorption (per min).

The values for C_o, C_x, and Q are established by the experimental test conditions, as is the constant temperature. The value of ρ_β—which is dependent on the fill weight, granular size, shape of the adsorbent, and fill volume—can be determined experimentally and is part of the manufacturer's production criteria.

Thus, if one conducts experiments using charcoal beds of different weight and determines the breakthrough time (t_b), values for W_e and k_v can be calculated from Equation (1). Rewriting Equation (1) yields the following form:

$$t_b = \frac{W_e W}{C_O Q} - \frac{W_e \rho_\beta}{k_v C_O}\mathrm{Ln}(C_O/C_X) \quad (2)$$

If one plots the breakthrough time (t_b) as a function of the bed weight (W), a straight line results where the slope and intercept allow calculation of the adsorption capacity and adsorption rate constant. The slope is equal to W_e/C_oQ. The y-axis intercept is equal to

$$\frac{-W_e \rho_\beta}{k_v C_O}\mathrm{Ln}(C_O/C_X) \quad (3)$$

and the x-axis intercept W_c (critical bed weight) is equal to $\rho_\beta Q\ \mathrm{Ln}(C_o/C_x)/k_v$. By knowing the slope, a value for W_e (adsorption capacity) can be determined. By inserting W_e into the y-axis intercept relationship, one can calculate the adsorption rate constant k_v.

RESULTS

It has been reported[7] that these chemiresistor sensors' responses might change with exposure; thus, the data are presented in chronological order. The first set of three experiments (runs 1, 2, and 3) were run employing a normal ethyl acetate challenge concentration of 1000 ppm.

The t_b at the normal challenge concentration was obtained by multiplying the experimentally determined t_b by C experimental/C normal. The data are presented in Table I. Figure 3 illustrates the IR and microsensor responses as a function of exposure time to the challenge vapor. The data clearly indicate that the chemiresistor sensors detected breakthrough, and that the sensors were capable of being developed as active EOSLI. It can be seen that the sensors were

TABLE II. Wheeler Constants for Ethyl Acetate Challenge Vapor at 1, 5, and 10% Breakthrough for Lot B

Corrected Challenge Conc. (ppm)	% t_b	# Pts.	% RH	Slope	Y Axis Intercept	R^2	Average Bed Bulk Density (ρ_B) g/cm^3	W_e Kinetic Adsorption Capacity (g/g)	k_v Rate Constant (min^{-1})	W_c Critical Bed Weight (g)
750	1	8	50	1.257	−25.05	0.993	0.442	0.218	6540	19.93
	5	8	50	1.260	−17.40	0.992	0.442	0.218	6140	13.81
	10	8	50	1.264	−13.42	0.992	0.442	0.219	6140	10.62
1000	1	12	50	1.018	−16.72	0.999	0.438	0.235	7860	16.42
	1	12	50	0.976	−21.91	0.997	0.449	0.225	5900	22.44
	5	12	50	1.020	−10.71	0.999	0.438	0.235	8000	10.50
	5	12	50	0.983	−16.03	0.997	0.449	0.227	5280	16.31
	10	12	50	1.021	−8.15	0.999	0.438	0.235	8080	7.99
	10	12	50	0.983	−12.99	0.997	0.449	0.227	5010	13.21
1500	1	8	50	0.762	−14.27	0.995	0.437	0.264	6870	18.73
	5	8	50	0.762	−9.82	0.994	0.437	0.264	6500	12.89
	10	8	50	0.765	−8.22	0.994	0.437	0.265	5980	10.75
2000	1	8	50	0.594	−11.72	0.997	0.438	0.274	6540	19.74
	5	8	50	0.596	−8.38	0.997	0.438	0.275	5960	14.08

not as sensitive as the IR detector and/or possessed a slower response time. Further, the sensors exhibited significantly more background noise and drift, which must be overcome.

Initially, the IR data was plotted in accordance with the modified Wheeler equation (Equation 1). When breakthrough time was plotted as a function of charcoal weight, a linear relationship was observed.[8] The correlation values (R^2 equaled 0.999 at 1% t_b for a 1000 ppm challenge) and values for the Wheeler constants at different breakthrough percentages are given in Table II. Likewise, the sensor data should conform to the modified Wheeler equation if all the sensors have essentially the same response factor. As anticipated, a linear relationship does exist between breakthrough time (determined at the midpoint of the sensors' total response) and sorbent weight for the first three sensors (9 points) for the 1000 ppm challenge. Sensor 4's deviation was attributed to its significantly enhanced sensitivity over the other three sensors. The equation of this line was determined to be $t_b = 1.134\ W + 2.9992$, and the R^2 value was 0.960. If one substitutes the IR t_b values for the cartridges at some arbitrary level—say 100 ppm breakthrough—into this sensor equation, one can determine the charcoal bed depth position for the sensor, assuming that they are sensitive enough to detect the 100 ppm level. These calculated values are given in Table I. It can be seen that the position of the sensor in the first cartridge would be approximately 75% of the way into the charcoal bed.

The second set of two experiments (runs 4 and 5) were performed at a 1500 ppm ethyl acetate challenge concentration. The breakthrough data for both the IR and sensors are given in Table III. Again, a linear relationship exists between breakthrough time and sorbent weight (Table II gives Wheeler constants for the IR data). The sensor breakthrough time (midpoint response) versus sorbent weight was linear

TABLE III. Organic Vapor Cartridge Breakthrough Time (t_b) Against 1500 ppm Ethyl Acetate for Stacked Cartridges[A]

Run #	Filter # in Stacked Array	Cumulative Charcoal WT (g)	IR t_b Corrected to 1500 ppm (min) at Various Penetration				t_b to Midpoint of Sensor Response (min)	W[B] Charcoal Bed Weight Needed for 100 ppm (g)	$W_{\%}$[C] % of Bed Where Sensor to be Located
			15 ppm	75 ppm	100 ppm	150 ppm			
4	1	68.304	38.9	43.8	44.7	45.4	71	44.9	63
	2	138.135	95.1	99.4	100.1	101.2	122	111.7	78
	3	208.222	149.5	154.5	155.3	157.0	182	178.2	84
	4	279.369	203.7	208.9	209.8	211.5	214	243.9	86
5	1	70.154	37.1	41.2	42.0	43.0	58	41.7	61
	2	140.183	89.2	93.8	94.6	95.9	125	105.1	76
	3	209.547	141.2	145.4	146.3	147.3	179	167.4	80
	4	279.567	192.6	196.7	197.4	198.4	207	228.9	83

[A]Carbon Bed Density 0.44 g/cm^3

[B] $W = \frac{t_b - 7.4072}{0.8299}$

[C] $W_{\%} = \frac{W}{W_{cum}}(100)$

TABLE IV. Organic Vapor Cartridge Breakthrough Time (t_b) Against 2000 ppm Ethyl Acetate for Stacked Cartridges[A]

Run #	Filter # in Stacked Array	Cumulative Charcoal WT (g)	IR t_b Corrected to 2000 ppm (min) at Various Penetration		t_b to Midpoint of Sensor Response (min)	W[B] Charcoal Bed Weight Needed for 100 ppm (g)	$W_{\%}$[C] % of Bed Where Sensor to be Located
			20 ppm	100 ppm			
6	1	71.077	29.9	33.5	47	44.0	62
	2	142.394	70.2	73.8	95	98.7	69
	3	213.432	112.9	116.8	149	157.1	74
	4	283.748	153.0	157.0	165	211.7	75
7	1	68.414	29.3	33.1	49	43.4	64
	2	137.941	71.9	75.2	117	100.6	73
	3	208.066	115.2	118.5	156	159.4	77
	4	276.649	155.9	159.9	167	215.6	78

[A]Carbon bed density 0.44 g/cm^3

[B]$W = \frac{t_b - 1.1074}{0.7365}$

[C]$W_{\%} = \frac{W}{W_{cum}}(100)$

and the equation of the line for the first three sensors was $t_b = 0.8299\ W + 7.4072$ ($R^2 = 0.991$). Again, inserting the IR t_b values for the cartridges at an arbitrary level of 100 ppm breakthrough allows us to determine the charcoal bed depth for these sensors. The calculated values are shown in Table III. The calculated position of the sensor in the first cartridge would be approximately 60% of the way into the charcoal bed, and the sensor would alarm when 100 ppm cartridge breakthrough occurred.

The third set of data (runs 6 and 7) was done at 2000 ppm of an ethyl acetate challenge. The breakthrough data for both detector systems are presented in Table IV (Table II gives Wheeler constants for the IR data). The sensor breakthrough time versus sorbent weight (first three sensors, six points) can be described by the linear equation $t_b = 0.7365\ W + 1.1074$ ($R^2 = 0.962$). Going through the same calculations, using the 100 ppm level, gives the charcoal bed depth for the sensors as shown in Table IV. The position of the sensor in the first cartridge was approximately 60% into the charcoal bed.

Approximately 3 months after the initial 1000 ppm sample runs, another set of 1000 ppm ethyl acetate runs were performed to check the stability of the sensors with time. The breakthrough data and bed depth calculations are presented in Table V. On evaluation of this data, it was obvious that the sensors had remained stable, though the intensity of the response appeared to have diminished somewhat. The linear response between t_b and charcoal weight for the first three sensors gave an equation of $t_b = 1.1181\ W - 1.4726$ and the R^2 value 0.990 (Table II gives the IR Wheeler constants). This correlates well with the first set's equation of $t_b = 1.134\ W + 2.9992$ ($R^2 = 0.971$); the combined data

TABLE V. Three Month Sensor Stability Evaluation Against 1000 ppm Ethyl Acetate for Stacked Cartridges[A]

Run #	Filter # in Stacked Array	Cumulative Charcoal WT (g)	IR t_b Corrected to 1000 ppm (min) at Various Penetration			t_b to Midpoint of Sensor Response (min)	W[B] Charcoal Bed Weight Needed for 100 ppm (g)	$W_{\%}$[C] % of Bed Where Sensor to be Located
			10 ppm	50 ppm	100 ppm			
8	1	72.159	52.4	58.3	61.1	82	56.0	77
	2	144.267	121.9	128.4	131.9	168	119.3	83
	3	215.558	190.7	198.0	201.7	—	181.7	84
	4	287.729	265.8	273.3	277.9	279	249.9	87
9	1	72.614	48.7	55.9	59.4	80	54.4	75
	2	145.392	119.9	126.7	128.9	160	116.6	80
	3	218.537	191.4	199.0	201.3	232	181.4	83
	4	289.835	264.5	272.5	274.1	276	246.5	85
10	1	71.559	48.2	54.3	57.5	72	52.7	74
	2	143.407	111.2	117.7	121.2	158	109.7	76
	3	212.246	180.9	187.9	191.3	244	172.4	81
	4	284.700	248.6	256.0	260.0	263	233.9	82

[A]Carbon Bed Density 0.45 g/cm^3

[B]$W = \frac{t_b - 1.4726}{1.1181}$

[C]$W_{\%} = \frac{W}{W_{cum}}(100)$

TABLE VI. Organic Vapor Cartridge Breakthrough Time (t_b) Against 750 ppm Ethyl Acetate for Stacked Cartridges[A]

Run #	Filter # in Stacked Array	Cumulative Charcoal WT (g)	IR t_b Corrected to 750 ppm (min) at Various Penetration				t_b to Midpoint of Sensor Response (min)	W[B] Charcoal Bed Weight Needed for 100 ppm (g)	$W_{\%}$[C] % of Bed Where Sensor to be Located
			7.5 ppm	37.5 ppm	75 ppm	100 ppm			
11	1	72.985	66.5	74.2	78.3	80.4	87	58.3	80
	2	145.025	150.9	158.3	162.5	163.8	208	115.7	80
	3	216.924	235.6	244.1	248.9	250.4	297	175.3	81
	4	283.498	321.2	329.1	333.8	334.7	336	233.3	82
12	1	70.965	65.1	73.4	78.1	80.2	100	58.2	82
	2	143.347	161.2	169.2	173.5	175.4	229	123.7	86
	3	213.420	253.3	261.5	266.4	268.6	307	187.8	88
	4	282.729	342.5	351.4	357.1	360.0	—	250.7	89

[A]Carbon Bed Density 0.44 g/cm^3

[B] $W = \frac{t_b + 4.4100}{1.4538}$

[C] $W_{\%} = \frac{W}{W_{cum}}(100)$

equation was $t_b = 1.1290\ W + 0.5988$. Since both sets of data are comparable, this confirmed the stability of these sensors for repeated use over the 3-month period.

A final set of data was collected at a challenge concentration of 750 ppm ethyl acetate. The breakthrough data are presented in Table VI. With this set of data, the signal-to-background sensor drift created some difficulties. However, the same data trends were observed. The sensor equation was found to be $t_b = 1.4538\ W - 4.4100$ with an R^2 value of 0.977 (Table II gives the Wheeler constants for the IR system). The bed depth calculations using an IR 100 ppm breakthrough concentration level are presented in Table VI.

Finally, if one plots the 10% infrared breakthrough time versus the chemiresistor microsensor midpoint breakthrough time (Figure 4), one observes a linear relationship. The correlation factor (R^2 of 0.9619) indicates excellent correlation, and suggests that the two detector systems are measuring the same contaminant breakthrough phenomenon. However, the microsensor response lags behind the IR detector response by approximately 20–25 min as indicated by the intercept in Figure 4. This is attributed to detector sensitivity and/or response time of the microsensor/data logger system.

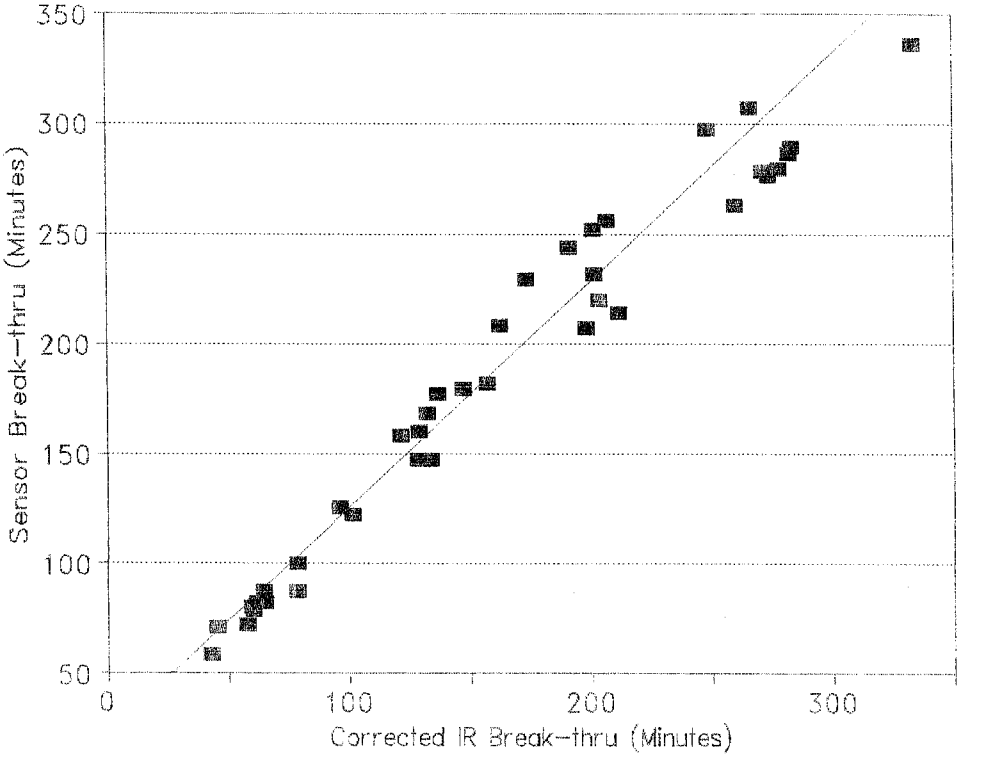

FIGURE 4. Plot of infrared detector breakthrough time at 10% penetration versus breakthrough time of microsensors at midpoint response

CONCLUSIONS

A small, low cost, lightweight, and micro-power carbon-based chemiresistor microsensor has been developed and shown to detect OV cartridge breakthrough. The data indicate that the sensors would probably have to be located inside the carbon bed; this position would have the added advantage of having the sensors experience a reduced relative humidity and rather clean environment. These observations indicate that chemiresistor microsensors have potential applicability as active EOSLI. However, development and validation of these devices, according to the NIOSH criteria for certification of EOSLI,[11] will be a lengthy process.

A further area for research would be improvement in sensor sensitivity. In this regard, one of the sensors showed a significantly higher detector response than did the other three. This suggests that the detectors have not been optimized, and optimization would enhance their potential use characteristics. Further, the optimization of the sensor is desirable since the PELs of many organic compounds are being lowered. Also, although ethyl acetate was the only contaminant studied, these sensors should respond to any organic compound that swells the sensor matrix. In fact, it has been shown that nonpolar compounds are detected more efficiently than polar compounds, which is consistent with Theta[12,13] solvent behavior.

These experiments showed that the sensors are reusable, and that they stabilize quickly after an experimental run. However, the baseline stability of the sensors needs to be enhanced. Variations of resistance, whether due to flow rate fluctuations, temperature, or relative humidity, must be overcome. It was thought that the use of a reference sensor arrangement would overcome this problem, but it is not a simple matter to isolate, identify, and correct drift problems. Environmental factors like relative humidity, cyclic flow patterns, and large temperature fluctuations, which would be seen under field applications, could add to sensor drift.

When these sensors are uniformly produced, so as to maintain a constant response factor, they could be used as active EOSLI in OV cartridges to assist with administrative control procedures with negative-pressure respirator equipment. Further, sensor development and use as personal monitors might be a meaningful, useful application.

REFERENCES

1. "Mineral Resources," *Code of Federal Regulations*, Title 30, Part 11, Subpart I—Gas Masks 88 11.90, Footnote 4. 1980. p. 36.
2. "Mineral Resources," *Code of Federal Regulations*, Title 30, Part 11, Subpart 2—Chemical Cartridge Respirators 88 11.150, Footnote 8. 1980. p. 58.
3. **National Institute for Occupational Safety and Health:** *Respirator Decision Logic.* (NIOSH/DHHS Pub. No. 87-108). Washington, D.C., U.S. Government Printing Office, 1987.
4. **Moyer, E.S.:** Review of Influential Factors Affecting the Performance of Organic Vapor Air-Purifying Respirator Cartridges. *Am. Ind. Hyg. Assoc. J. 44*:46–51 (1983).
5. **Amoore, J.E. and E. Hautala:** Odor as an Aid to Chemical Safety: Odor Thresholds Compared with Threshold Limit Values and Volatilities for 214 Industrial Chemicals in Air and Water Dilution. *J. Appl. Toxicol. 3(6)*:272–290 (1983).
6. **TRC Environmental Consultants:** *Odor Thresholds for Chemicals with Established Occupational Health Standards.* Akron, Ohio: American Industrial Hygiene Association, 1989.
7. **Maclay, G.J., C. Yue, M.W. Findlay, and J.R. Stetter:** A Prototype Active End-of-Service-Life Indicator for Respirator Cartridges. *Appl. Occup. Environ. Hyg. 6(8)*:677–682 (1991).
8. **Moyer, E.S.:** Organic Vapor (OV) Respirator Cartridge Testing—Potential Jonas Model Applicability. *Am. Ind. Hyg. Assoc. J. 48*:791–797 (1987).
9. **Wood, G.O. and E.S. Moyer:** A Review of the Wheeler Equation and Comparison of its Applications to Organic Vapor Respirator Cartridge Breakthrough Data. *Am. Ind. Hyg. Assoc. J. 50*:400–407 (1989).
10. **Rehrmann, J.A. and L.A. Jonas:** Dependence of Gas Adsorption Rates on Carbon Granule Size and Linear Flow Velocity. *Carbon 16*:47–51 (1978).
11. "Notice of Acceptance of Applications for Approval of Air Purifying Respirators with End-of-Service-Life Indicators (ESLI)." *Federal Register 49*:140 (19 July 1984) pp. 29271–29272.
12. **Van Krevelen, D.W. and P.J. Hoftyzer:** *Properties of Polymers.* 2nd ed. New York: Elsevier Scientific Publishing Co., 1976. pp. 174–175.
13. **Brandrup, J. and E.H. Immergut:** *Polymer Handbook.* 2nd ed., New York: John Wiley and Sons, 1975. pp. 157–159.